IEEE Access
Multidisciplinary | Rapid Review | Open Access Journal

Received 24 October 2022, accepted 4 November 2022, date of publication 7 November 2022, date of current version 16 November 2022.

Digital Object Identifier 10.1109/ACCESS.2022.3220672

RESEARCH ARTICLE

Low RCS Dual-Polarized Crossed Dipole Antenna Co-Designed With Absorptive Frequency-Selective Reflection Structure

MEHRAN MANZOOR ZARGAR[1], (Graduate Student Member, IEEE), ARCHANA RAJPUT[2], KUSHMANDA SAURAV[1], (Member, IEEE), AND SHIBAN K. KOUL[3], (Life Fellow, IEEE)

[1]Department of Electrical Engineering, Indian Institute of Technology Jammu, Jammu, Jammu and Kashmir 181221, India
[2]Department of Electronics and Communication Engineering, National Institute of Technology Srinagar, Srinagar, Jammu and Kashmir 190006, India
[3]Centre for Applied Research in Electronics, Indian Institute of Technology Delhi, New Delhi 110016, India

Corresponding author: Mehran Manzoor Zargar (mehzargar@yahoo.com)

This work was supported by the Directorate of Extramural Research and Intellectual Property Rights (DER and IPR), Defence Research and Development Organisation (DRDO), Ministry of Defence, Government of India, through the Project title ''Studies of the Design of Microwave Structures for Achieving Low RCS of Dielectric and Conducting Objects,'' under Grant ERIP/ER/202207004/M/01/1808.

ABSTRACT This article proposes a novel strategy for realizing a reduction in radar cross-section (RCS) of dual-polarized crossed dipole antenna. At first, a compact and polarization-insensitive absorptive frequency-selective reflection (AFSR) structure is proposed by incorporating a bandstop ring resonator within the circular-cross based broadband absorber. The bandstop ring resonator is designed on the backside of the resistive layer due to which a reflection window is realized at a frequency of 8.2 GHz between the two broadband absorptions (4.2−7.0 GHz and 9.2−11.5 GHz). A dual-polarized crossed dipole antenna is designed with operating frequency lying within the reflecting notch of the AFSR structure. A 6 x 6 AFSR structure array is truncated at the center where from which the crossed dipole is connected through a feed substrate. The AFSR structure enacts as a modified ground plane to the crossed dipole antenna. The proposed AFSR integrated antenna achieves an average mono-static RCS reduction of 12.51 dB and 12.62 dB for the TE and TM incident waves, respectively. Further, the AFSR based antenna is also measured for the bi-static RCS, wherefrom the average total RCS reduction of 80% for TE and TM incidence is attained in the frequency band of 4.2 to 11.5 GHz.

INDEX TERMS Absorptive frequency-selective reflection, frequency-selective surface, polarization-insensitive.

I. INTRODUCTION

The detectability reduction of the target from the radar system is a vital aspect of stealth technology. In recent years, studies involving the development of radiating systems exhibiting low radar cross-section (RCS) have gained a great deal of attention. RCS which quantifies the detectability parameter of the target should have the minimum value for enhancing the secrecy factor of the target in stealth technology [1]. Thus, the RCS of the radiating system employed in the stealth technology is of key consideration. In the literature, several approaches for the realization of low RCS radiating systems have been reported. Some of these reported techniques include geometrical shaping of antennas [2], [4], applying radar absorbing materials [5], [7], utilization of polarization converter structures [8], [9], and usage of surfaces involving artificial magnetic conductor [10], [11]. However, in the reported techniques several drawbacks like poor radiation, narrowband RCS reduction with angle based low RCS are also accompanied.

The advent of absorptive frequency-selective reflection (AFSR) type structure has serve for a substantial application in the realization of a low RCS antenna system [12], [13]. The AFSR structure is a specialized category of frequency-selective surface (FSS), which features a notch shaped reflection band along with one-/two-sided absorption bands.

The associate editor coordinating the review of this manuscript and approving it for publication was Chinmoy Saha.

A suitable integration of the ASFR structure with the antenna can be effective in realizing a system with low out-of-band RCS. In the recent past several studies on the AFSR structures have been reported in the literature [14] and [19]. A band notched AFSR structure using circular slot resonator and metal strip resonator has been reported in [14]. A polarization-insensitive AFSR using multiple resonators has been proposed in [15]. A triple-layered polarization insensitive AFSR structure with reflectance band centered at 5 GHz has been proposed in [16].

Recently various studies on the RCS reduction techniques have been reported [20], [30], that includes realization of low RCS antenna using AFSR structure [23], [24]. In [23], a dipole antenna is studied with a single-polarization AFSR structure realizing a reduction in out-of-band RCS. Low RCS monopole and dipole antennas have been studied in [24], by integrating with a 3-D AFSR structure based on multimode resonators. The AFSR structure exhibiting polarization-insensitive behavior can have a suitable application for RCS reduction of the radiating system operating in dual polarization.

The objective aimed in this work is to study the integration strategy of a dual-polarized crossed dipole antenna with a polarization-insensitive AFSR structure for achieving RCS reduction. A brief preliminary study of this work has been presented in [31] in which a mono-static RCS reduction of a single polarized dipole antenna is discussed using the proposed ASFR structure. In comparison with the initial work [31], the study carried out for the extended work in this paper includes the experimental validation of the AFSR structure along with the corresponding equivalent circuit model. Further, the extended work in this paper in contrast to the initial work [31], employs a dual-polarized crossed dipole antenna integrated which is more suitable than a single-polarization dipole antenna integrated with the polarization-insensitive AFSR structure. Further, the mono-static RCS in this extended paper, unlike the initial work [31], is experimentally determined. Furthermore, in this extended work, the bi-static measurements are also performed. The novelties achieved in the proposed work are enlisted as:

- Design of the 2-D polarization-insensitive AFSR structure by subtle idea of printing a circular ring resonator on the back of the front resistive substrate which achieves a reflection notch (at 8.2 GHz) with the adjacent side absorption bands (4.2-7.0 GHz and 9.2-11.5 GHz) on both side. The design complexity of the proposed AFSR is much lesser as compared to asymmetric AFSR design of [14], 3-layer design of [16] and 3D AFSR structures reported in [17] and [19].
- Integration of a crossed dipole antenna with a 6 x 6 proposed AFSR structure unit cells in a novel and proficient manner such that AFSR structure acts as a reflector at the antenna's operating frequency. The proposed work realizes a dual-polarized low RCS antenna in contrast to the single-polarized antennas reported in [23] and [28].

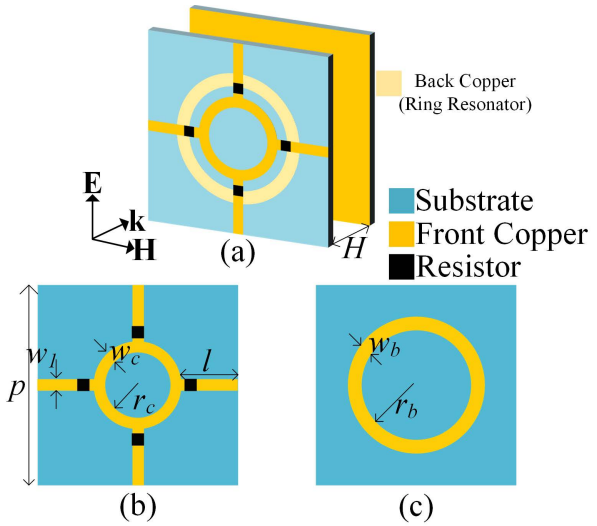

FIGURE 1. AFSR unit cell geometry, (a) perspective view, (b) front side, and (c) back side of top resistive layer. Dimensions (in mm): $p = 15$, $r_c = 2.2$, $w_c = 1$, $r_b = 3.2$,$w_1 = 0.8$, $w_b = 0.6$, $l = 4.3$, and $H = 8$.

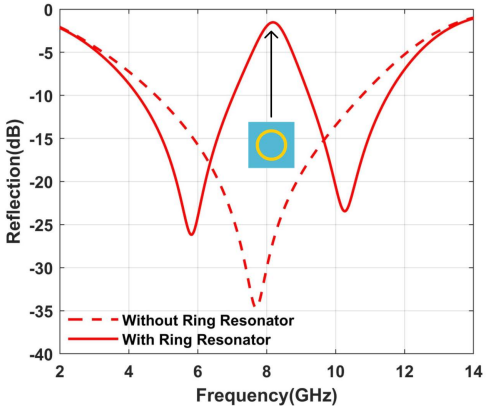

FIGURE 2. Simulated reflection coefficients of the AFSR structure and the broadband absorber.

- The mono-static RCS of the AFSR integrated antenna achieves an average reduction of 12.51 dB and 12.62 dB for the TE and TM incidence, respectively in comparison with the conventional reflector back antenna.
- In contrast to the reported works [23], [29], the bi-static measurement on the proposed AFSR antenna is carried out at different angles for obtaining the normalized total scattered cross section. An average bi-static total RCS reduction of 80.2% is exhibited for both TE and TM incident wave as compared to the conventional reflector back antenna.

The paper is organized in the sequence given. Section II discusses the AFSR structure including analysis and experimental validation. Section III presents the integration technique of crossed dipole with the AFSR structure for both mono-static and bi-static RCS reduction. Finally, conclusion is provided in section IV.

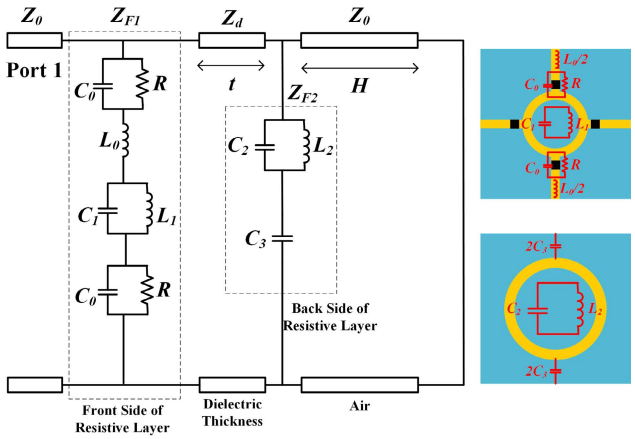

FIGURE 3. ECM of the proposed AFSR structure ($R = 200\Omega$, $C_0 = 0.051$ pF, $L_0 = 2.45$ nH, $C_1 = 0.0011$ pF, $L_1 = 3.185$ nH, $C_2 = 0.1$ fF, $L_2 = 39.305$ nH, $C_3 = 0.0091$ pF, $Z_d = 181\ \Omega$, $t = 0.8$ mm, $Z_0 = 377\ \Omega$).

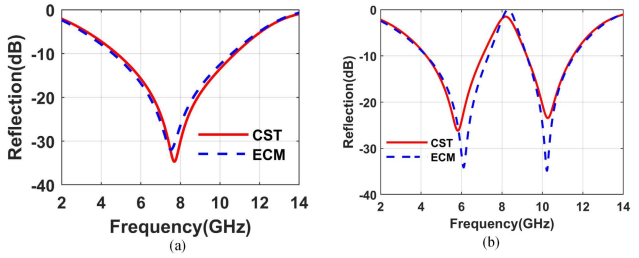

FIGURE 4. ECM response in comparison with the CST results. (a) Broadband absorber, and (b) AFSR structure.

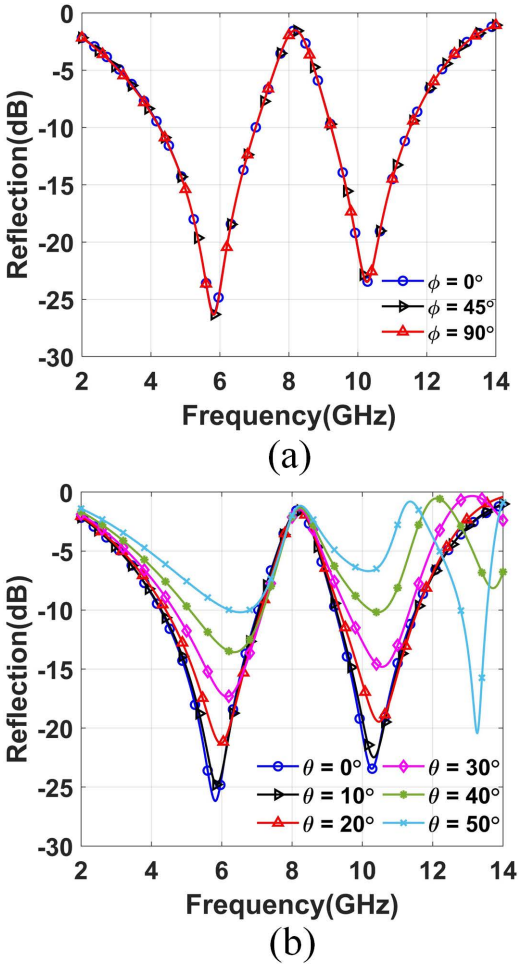

FIGURE 5. Simulated responses of the proposed AFSR structure with respect to different (a) polarization, and (b) incidence angle.

II. AFSR STRUCTURE

A. DESIGN AND ANALYSIS

The geometrical discription of the proposed unit cell for the ASFR structure is depicted in Fig. 1, which is basically a two-layered combination comprising of resistive layer at top and ground layer at bottom and separated by distance H (Fig. 1(a)). The design is printed on a 0.8 mm thick FR-4 substrate. The resistive layer comprises of a circular-cross shaped resonator on the front side in which the lumped chip resistors having resistance of 200 Ω are mounted within the four gaps of the rectangular strip (Fig. 1(b)). On the backside of the resistive layer a metallic circular ring resonator is printed. The CST Microwave studio is used for analyzing the structure.

The resistive layer with circular-cross resonator and lumped chip resistors placed from the ground layer at a distance of $\lambda/4$ provides a broadband absorption for the incident EM wave as shown in Fig. 2 and having 90% absorption bandwidth from 4.7 to 10.7 GHz. For obtaining a reflection notch in middle of the absorption band a metallic circular ring is printed on the backside of the resistive layer. This circular ring resonator acts as a bandstop FSS at the desired reflection notch of 8.2 GHz. It can be observed from Fig. 2 that due to insertion of ring resonator at the back side of resistive layer the broad absorption band gets bifurcated into two absorption bands from 4.2 to 7.0 GHz and 9.2 to 11.5 GHz with a notch shaped reflection band at the center frequency of 8.2 GHz.

For understanding the working related to the proposed AFSR structure, a corresponding equivalent circuit model (ECM) is designed as shown in Fig. 3. The ECM is a one-port network in which the corresponding models of front and back side resonators of the resistive layers are cascaded. For the circular-cross resonator at the front side, the lumped resistor and the associated gap capacitance is modelled by the parallel $R - C_0$ combination. The inductance of the rectangular strip is modelled by inductor L_0 while the parallel $L_1 - C_1$ models the circular ring. At the backside of resistive layer, the circular ring is modelled by the parallel $L_2 - C_2$ while the inter-capacitance is represented by C_3. The thickness of the substrate is modelled by a transmission line having the characteristic impedance $Z_d = Z_0/\sqrt{\epsilon_r}$ (Z_0 denotes the impedance in free space) and length equivalent to the substrate thickness (t). The transmission line having characteristic impedance Z_0 and thickness H also models the air-gap between the resistive layer and the ground.

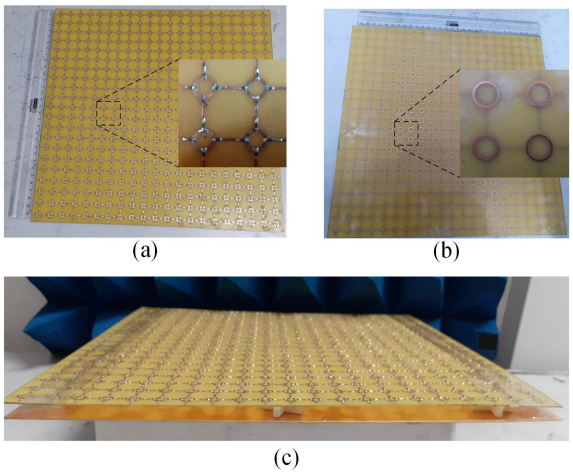

FIGURE 6. Photograph of the fabricated AFSR prototype. (a) Front, and (b) back side of the top layer. (c) Side view.

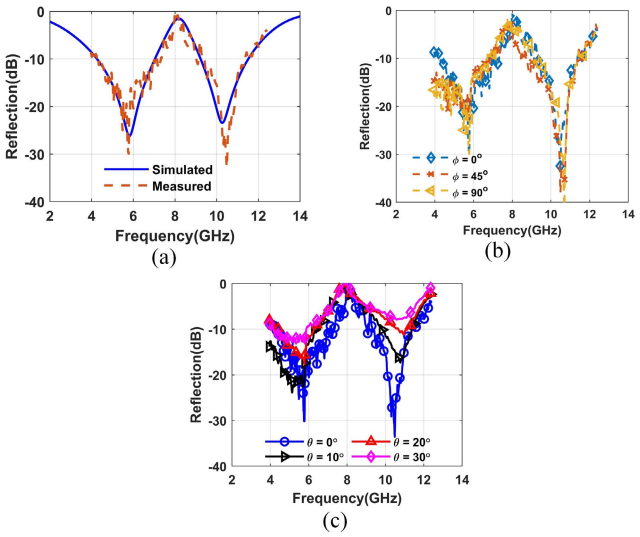

FIGURE 7. Measured reflection coefficients for the proposed AFSR structure (a) in comparison with the simulated result, (b) under different polarization, and (c) oblique incidence.

The Keysight ADS solver is used for analyzing the ECM of the proposed AFSR structure. The simulated reflection coefficient of the ECM compared with the full wave CST simulation is shown in Fig. 4. The response of the ECM without the backside ring resonator model is shown in Fig. 4(a), in which a broadband absorption is observed in close resemblence with the full wave simulation of the broadband absorber. The reflection of the ECM for AFSR is shown in Fig. 4(b) in which the reflection notch at the center is achieved by the addition of corresponding model of the backside ring resonator. The close concurrence between the ECM and CST responses explains the working of the AFSR design.

The proposed AFSR structure is analyzed in response to multiple polarization angles associated with the incident EM wave as depicted in Fig. 5(a). The consistent response of the design under various polarization angles determines the

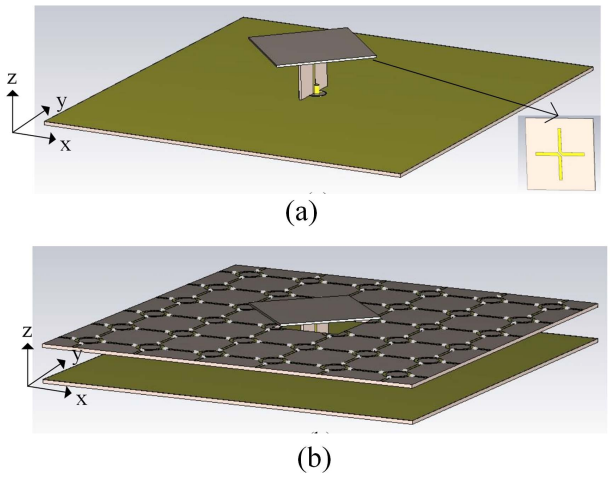

FIGURE 8. Schematic representation of the crossed dipole antenna with (a) reflector, and (b) AFSR structure.

polarization-insensitive behavior of the AFSR structure. Furthermore, the AFSR structure is also analyzed corresponding to the oblique angle of incidence up to 50^o. The angular stability for the proposed structure exists up to 30^o beyond which the absorption bands gets degraded.

B. FABRICATION AND MEASUREMENTS

For obtaining the experimental validation of the AFSR structure, a prototype consisting of 21 x 21 proposed unit cells are fabricated using a 0.8 mm thick FR-4 substrate ($\epsilon_r = 4.4$, $tan\delta = 0.02$). The photograph of the fabricated prototype having overall size of 315 mm x 315 mm is given in Fig. 6. Lumped chip resistors with 200 Ω resistance (CRCW0603200RFKEA from VISHAY) are soldered within the gaps of the circular-cross resonators (Fig. 6(a)). The metallic ring resonators are printed on the backside of the top resistive layer (Fig. 6(b)). The resistive substrate is separated from the ground layer using a plastic spacers as presented in Fig. 6(c).

The reflection measurements on the fabricated prototype is carried in an anechoic chamber using the free space technique with standard gain horn antennas of C, J and X bands in connection with the Keysight PNA N5224B. The measured reflection coefficient of the fabricated prototype in comparison with the simulated response is shown in Fig. 7(a). The close resemblance achieved between the experimental and simulated responses validates the proposed design experimentally. Further, the polarization-independence of the proposed structure is also experimentally validated by measuring the response at various polarization angles as shown in Fig. 7(b). The response of the proposed structure is measured under oblique incidence and the angular stability is experimentally validated up to 30°, beyond which the absorptivity in the two bands gets degraded.

III. LOW RCS CROSSED DIPOLE ANTENNA

The design for the dual-polarized low RCS antenna utilizing the AFSR structure is proposed in this section. The AFSR

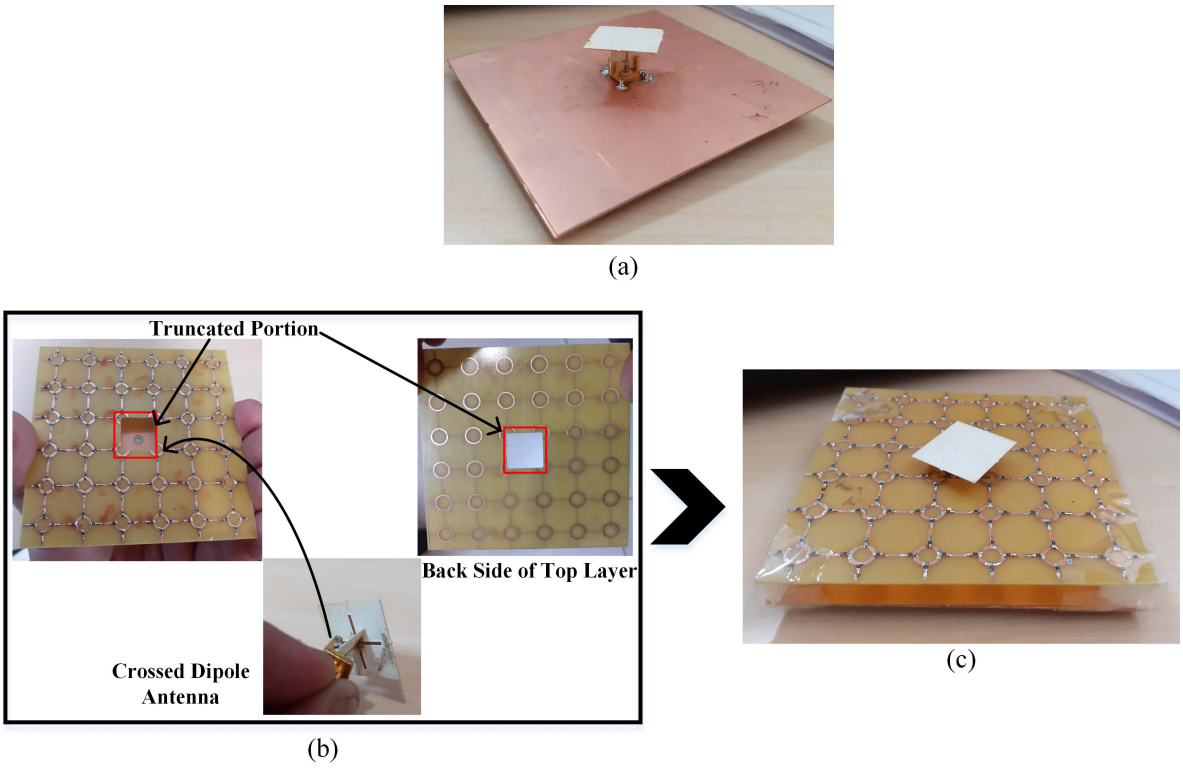

FIGURE 9. Photographs of the fabricated prototype of the crossed dipole antenna with (a) reflector, (b) truncated 6 x 6 structure and (c) final AFSR structure.

structure exhibiting polarization-insensitive behavior is co-designed with the dual-polarized crossed dipole antenna. The crossed dipole antenna is designed having operating frequency around 8.2 GHz which corresponds to the reflection band associated with the proposed AFSR structure. A microstrip to broadside coupled stripline transition feeds the crossed dipole [32]. The reference structure consists of a crossed dipole backed by a metallic reflector as shown in Fig. 8(a). The dimension of the reflecting surface is taken to be equal with the size of 6 x 6 AFSR unit cell arrray (90 mm x 90 mm). In the design for AFSR integrated antenna, an array comprising of 6 x 6 unit cell is taken. On the resistive layer, a square portion with size of the order of the feed substrate is truncated at the center. The crossed dipole connected with the feed substrate as shown in Fig. 8(b), is inserted within this square portion and connected with the ground layer of the AFSR structure. In other words the grounded reflector of the antenna is modified with the 6 x 6 AFSR structure. The photographs showing the fabricated prototypes for the crossed dipole antenna with both metallic reflector and AFSR structure are depicted in Fig. 9.

The simulated and measured reflection coefficients (S_{11}) of the crossed dipole antenna with both reflector and AFSR structure are shown in Fig. 10. The reflection of less than -10 dB is observed at the operating frequency of 8.2 GHz for both the cases of reflector and ASFR backed antenna. At 8.2 GHz the gain of 5.52 dBi is observed for the

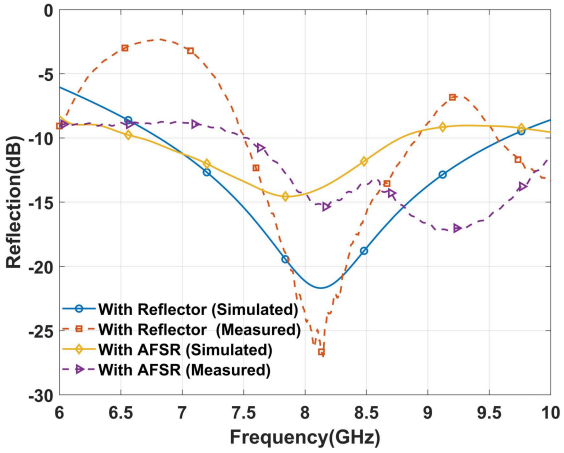

FIGURE 10. Reflection coefficient of the crossed dipole antenna.

AFSR backed antenna which is slightly less than the gain corresponding to reflector backed antenna (6.35 dBi). The simulated and measured radiation patterns of the crossed dipole antenna with both the reflector and AFSR backing in both the xz and yz planes are given in Fig. 11. It can be examined that the radiation pattern of the AFSR backed antenna is nearly similar as compare to the reflector backed antenna.

TABLE 1. Comparative performance of the proposed AFSR integrated antenna with the recently reported Low RCS antennas.

Ref.	Antenna Structure	Operating Frequency	Size	Lumped Elements in the structure	10 dB mono-static RCS bandwidth	Average Mono-static RCS reduction	Average Total Bi-static RCS reduction
[23]	Dipole + AFSR	8.7 GHz	3.65λ x 3.65λ	200	26% (Lower) and 16.7% (upper)	NA	NA
[24]	Monopole/Dipole + 3D AFSR	5.5 GHz	2.56λ x 1.54λ	196	64.7% (Lower) and 42.4% (upper)	NA	NA
[25]	Patch array antenna + AFST	10 GHz	7.2λ x 7.2λ	96	60.3% (Lower) and 20.4% (upper)	NA	NA
[26]	Patch antenna + Absorptive/Diffusive FSR	10 GHz	10.66λ x 10.66λ	512	90% (Lower) and 27.6% (upper)	NA	NA
[27]	Patch antenna + ASFT	7.5 GHz	1.5λ x 1.5λ	128	6.9% (Lower) and 39.3% (upper)	NA	NA
[28]	Slot array antenna + 3D AFST	6.15 GHz	1.96λ x 1.96λ	192	87.2% (Lower) and 45.8% (upper)	NA	NA
[29]	Cross-shaped Vivaldi antenna	1.8−6 GHz	0.58λ x 0.58λ	NA	NA	4.3 dB (TE) and 5 dB (TM)	NA
This Work	**Crossed dipole + AFSR**	**8.2 GHz**	**2.46λ x 2.46λ**	**144**	**38.59% (Lower-TE)/42.9% (Lower-TM) and 30.75% (upper-TE), 27% (Upper-TM)**	**12.51 dB (TE) and 12.62 dB (TM)**	**80 % (TE and TM)**

λ= wavelength at the operating frequency of antenna.

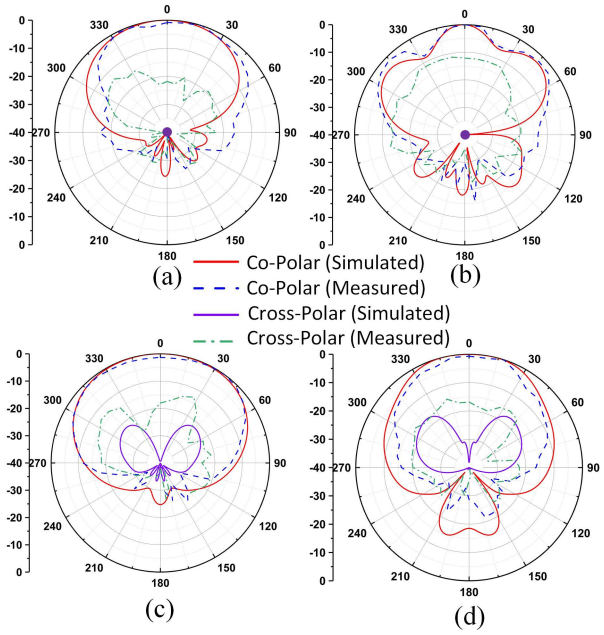

FIGURE 11. Radiation pattern of the crossed dipole antenna at 8.2 GHz. (a) xz plane (with reflector). (b) xz plane (with AFSR). (c) yz plane (with reflector). (d) yz plane (with AFSR).

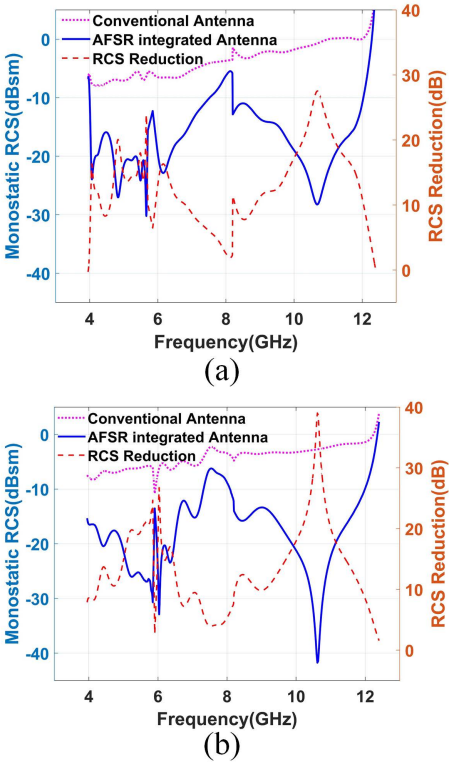

FIGURE 12. Mono-static RCS of the AFSR integrated antenna in comparison with the conventional reflector based antenna for (a) TE, and (b) TM incident wave.

A. MONO-STATIC RCS MEASUREMENT

The radar cross section measurements are carried out for the fabricated structures involving both the reflector and AFSR backed crossed dipole antennas. The Keysight PNA N5224B featured with time domain gating application is employed for the mono-static RCS measurement using the same standard gain horn antenna for both transmitter and receiver. The RCS is defined from the general equation by (1).

$$RCS = \frac{P_r}{P_t}.\frac{(4\pi)^3 R^4}{G_t G_r \lambda^2} = K.\frac{P_r}{P_t} \quad (1)$$

The terms P_r and P_t in (1) denote the received and transmitted powers, respectively. The gains associated with reflecting and transmitting antennas are represented by G_r and G_t, respectively. The range to target is given by R, whereas λ gives the associated wavelength.

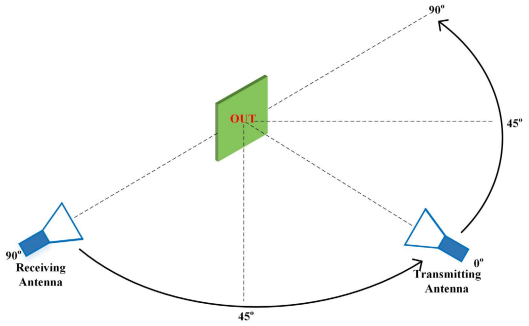

FIGURE 13. Schematic of experimental setup for bi-static measurement.

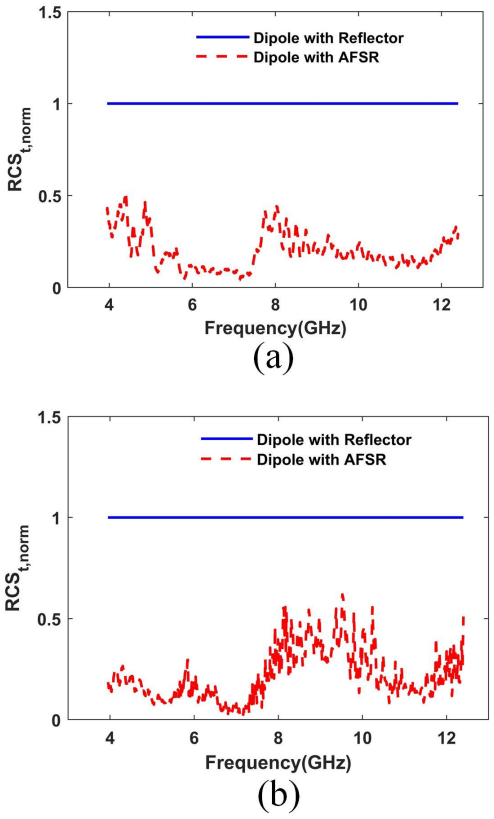

FIGURE 14. Normalised total bi-static RCS of the AFSR integrated antenna with reference to the conventional reflector based antenna for (a) TE, and (b) TM incident wave.

The mono-static RCS is measured in reference to a standard square PEC having same size as that of the grounded dimensions associated with antenna. The comparitive mono-static RCS of the metallic reflector and AFSR backed crossed dipole antenna for the TE and TM incident waves are shown in Fig. 12. It is observable that as compared with the reflector backed antenna, the AFSR integrated antenna achieves a low RCS with the maximum reduction of 27.52 dB (at 10.6 GHz) and 38.01 dB (10.6 GHz) for the TE and TM incidence, respectively. The AFSR integrated antenna achieves an average reduction of 12.51 dB and 12.62 dB for the TE and TM incident waves, within the frequency band extending from 4.2 to 11.5 GHz, respectively as compared to the conventional metallic reflector backed antenna.

B. BI-STATIC MEASUREMENT

The bi-static RCS measurement involves the transmitter and receiver test antennas placed at different locations. In the bi-static measurement, as depicted by Fig. 13, the transmitting antenna is normal to the structure while the receiving horn antenna is moved from 0^o to 90^0 along the circular path at 10^o steps in either anticlockwise or clockwise direction. The $E_{sca}(f, \phi)$ denoting the scattered field for each step angle is defined by (2) [33], [34].

$$E_{sca}(f, \phi) = S_{21,O}(f, \phi) - S_{21,FS}(f, \phi) \tag{2}$$

where the transmission coefficients between the two horn antennas corresponding to the object and free space are represented by $S_{21,O}$ and $S_{21,FS}$, respectively. The normalized total radar cross section $RCS_{t,norm}$ of the AFSR integrated antenna is calculated by the integrating scattered fields intensities as given in (3) [33]:

$$RCS_{t,norm} = \frac{\int |E_{sca,AFSRA}(f, \phi)|^2 d\phi}{\int |E_{sca,RA}(f, \phi)|^2 d\phi} \tag{3}$$

where $E_{sca,AFSRA}$ and $E_{sca,RA}$ are the scattered fields of the AFSR based and conventional reflector antennas, respectively.

The measured $RCS_{t,norm}$ for the AFSR combined crossed dipole antenna in reference with the metal reflector based antenna is provided in Fig. 14. It is noticed that with respect to the reflector based antenna, the AFSR structure based crossed dipole antenna achieves a significant reduction in the normalized total RCS. In the entire operating frequency band of 4.2 to 11.5 GHz, the average value of normalized RCS obtained is around 0.197 and 0.198 for the TE and TM incident wave, respectively which signifies a total RCS reduction of around 80.24% for both the TE and TM incidence, relative to the conventional reflector based crossed dipole antenna.

Table 1 presents the proposed AFSR integrated crossed dipole antenna with the other low RCS antennas reported in the literature. The proposed study presents the RCS reduction of dual-polarized crossed dipole antenna for the first time in comparison with the single polarization antennas reported [23], [28]. The proposed design is compact in comparison with reported work in [23], [25], and [26]. Further, the design complexity of the proposed structure is less than [23], [24], [26], and [28], in terms of lesser quantity of lumped components utilized. Also, the -10 dB RCS reduction bandwidth of the proposed design is more than [23] and [27] in the lower band while the RCS reduction bandwidth for the upper band is higher than the work reported in [23], [25], and [26]. The average RCS reduction achieved in the proposed design significantly higher in comparison with the reported work [29]. The proposed study achieves the RCS reduction using a 2D AFSR structure in comparison with the 3D FSS structures used in [24] and [28]. Furthermore, in

contrast to the reported works [23], [29], the scattered fields for the AFSR integrated antenna are measured in the proposed work at various angles and an average bi-static total RCS reduction of around 80% is experimentally demonstrated for both the TE and TM incident wave.

IV. CONCLUSION

In this study, a low RCS dual-polarized crossed dipole antenna is studied for the first time by judiciously integrating with a polarization-insensitive AFSR structure. The AFSR structure exhibiting a reflection notch (at 8.2 GHz) between the wide absorbing bands is designed by imprinting a bandstop ring shaped resonator on the back of the top resistive substrate. The crossed dipole antenna designed at the frequency concurrent with the reflecting notch of proposed AFSR structure, is adjusted within a small truncated area at the middle of the AFSR structure with 6 x 6 proposed unit cell array. The AFSR structure acts as a modified ground for the antenna. Both the mono-static and bi-static measurements performed on the dual-polarized antenna backed with the AFSR structure verify the RCS reduction while the other antenna parameters are observed to be maintained nearly the same. An average mono-static RCS reduction of 12.51 dB and 12.62 dB is acheived for the TE and TM incidence, respectively in the operating frequency band (4.2−11.5 GHz) for the AFSR based antenna compared with the conventional reflector comprising counterpart. Furthermore, an average total bi-static RCS reduction of around 80% is experimentally demonstrated in reference to the conventional reflector backed antenna. The proposed low RCS antenna is a potential candidate in the dual-polarized applications for stealth communication.

REFERENCES

[1] W. F. Bahret, "The beginnings of stealth technology," *IEEE Trans. Aerosp. Electron. Syst.*, vol. 29, no. 4, pp. 1377–1385, Oct. 1993.

[2] S. Hu, H. Chen, C. L. Law, Z. Shen, L. Zhu, W. Zhang, and W. Dou, "Backscattering cross section of ultrawideband antennas," *IEEE Antennas Wireless Propag. Lett.*, vol. 6, pp. 70–73, 2007.

[3] Y. B. Thakare, "Design of fractal patch antenna for size and radar cross-section reduction," *IET Microw., Antennas Propag.*, vol. 4, no. 2, pp. 175–181, Feb. 2010.

[4] W. Wang, S. Gong, X. Wang, Y. Guan, and W. Jiang, "Differential evolution algorithm and method of moments for the design of low-RCS antenna," *IEEE Antennas Wireless Propag. Lett.*, vol. 9, pp. 295–298, 2010.

[5] Y. Liu and X. Zhao, "Perfect absorber metamaterial for designing low-RCS patch antenna," *IEEE Antennas Wireless Propag. Lett.*, vol. 13, pp. 1473–1476, 2014.

[6] H. B. Baskey, E. Johari, and M. J. Akhtar, "Metamaterial structure integrated with a dielectric absorber for wideband reduction of antennas radar cross section," *IEEE Trans. Electromagn. Compat.*, vol. 59, no. 4, pp. 1060–1069, Aug. 2017.

[7] Y. Li, K. Zhang, L. Yang, and L. Du, "Wide-band radar cross-section reduction for antenna using frequency selective absorber," *Electron. Lett.*, vol. 52, no. 21, pp. 1809–1811, Oct. 2016.

[8] Y. Liu, K. Li, Y. Jia, Y. Hao, S. Gong, and Y. J. Guo, "Wideband RCS reduction of a slot array antenna using polarization conversion metasurfaces," *IEEE Trans. Antennas Propag.*, vol. 64, no. 1, pp. 326–331, Jan. 2016.

[9] Y. Liu, Y. Hao, K. Li, and S. Gong, "Radar cross section reduction of a microstrip antenna based on polarization conversion metamaterial," *IEEE Antennas Wireless Propag. Lett.*, vol. 15, pp. 80–83, 2016.

[10] Y. Zheng, J. Gao, X. Cao, Z. Yuan, and H. Yang, "Wideband RCS reduction of a microstrip antenna using artificial magnetic conductor structures," *IEEE Antennas Wireless Propag. Lett.*, vol. 14, pp. 1582–1585, 2015.

[11] Y. Zhao, X.-Y. Cao, J. Gao, and W. Q. Li, "Broadband RCS reduction and high gain waveguide slot antenna with orthogonal array of polarisation-dependent AMC," *Electron. Lett.*, vol. 49, no. 21, pp. 1312–1313, 2013.

[12] A. A. Omar, H. Huang, and Z. Shen, "Absorptive frequency-selective reflection/transmission structures: A review and future perspectives," *IEEE Antennas Propag. Mag.*, vol. 62, no. 4, pp. 62–74, Aug. 2020.

[13] Y. Han, Y. Chang, and W. Che, "Frequency-selective rasorbers: A view of Frequency-selective rasorbers and their application in reducing the radar cross sections of antennas," *IEEE Microw. Mag.*, vol. 23, no. 2, pp. 86–98, Feb. 2022.

[14] P. Mei, X. Q. Lin, J. W. Yu, and P. C. Zhang, "A band-notched absorber designed with high notch-band-edge selectivity," *IEEE Trans. Antennas Propag.*, vol. 65, no. 7, pp. 3560–3567, Jul. 2017.

[15] Y. Han, L. Zhu, Y. Chang, and B. Li, "Dual-polarized bandpass and band-notched frequency-selective absorbers under multimode resonance," *IEEE Trans. Antennas Propag.*, vol. 66, no. 12, pp. 7449–7454, Dec. 2018.

[16] A. Sharma, S. Ghosh, and K. V. Srivastava, "A polarization-insensitive band-notched absorber for radar cross section reduction," *IEEE Antennas Wireless Propag. Lett.*, vol. 20, no. 2, pp. 259–263, Feb. 2021.

[17] H. Huang and Z. Shen, "Low-RCS reflectarray with phase controllable absorptive frequency-selective reflector," *IEEE Trans. Antennas Propag.*, vol. 67, no. 1, pp. 190–198, Jan. 2019.

[18] B. Zhang, C. Jin, and Z. Shen, "Absorptive frequency-selective reflector based on bent metallic strip embedded with chip-resistor," *IEEE Trans. Antennas Propag.*, vol. 68, no. 7, pp. 5736–5741, Jul. 2020.

[19] B. Zhang, C. Jin, Q. Lv, J. Chen, and Y. Tang, "Low-RCS and wideband reflectarray antenna with high radiation efficiency," *IEEE Trans. Antennas Propag.*, vol. 69, no. 7, pp. 4212–4216, Jul. 2021.

[20] C. Jin, B. Zhang, L. Yin, Q. Lv, L. Kong, and L. Li, "Integrated low-profile low radar cross section circularly polarized dipole antenna array," *IEEE Trans. Antennas Propag.*, vol. 69, no. 12, pp. 8461–8469, Dec. 2021.

[21] T. Li, H. Yang, Q. Li, L. Jidi, X. Cao, and J. Gao, "Broadband low-RCS and high-gain microstrip antenna based on concentric ring-type metasurface," *IEEE Trans. Antennas Propag.*, vol. 69, no. 9, pp. 5325–5334, Sep. 2021.

[22] B. Wang, X. Q. Lin, Y. X. Kang, and R. X. Hu, "Low-RCS broadband phased array using polarization selective metamaterial surface," *IEEE Antennas Wireless Propag. Lett.*, vol. 21, no. 1, pp. 94–98, Jan. 2022.

[23] P. Mei, X. Q. Lin, J. W. Yu, A. Boukarkar, P. C. Zhang, and Z. Q. Yang, "Development of a low radar cross section antenna with band-notched absorber," *IEEE Trans. Antennas Propag.*, vol. 66, no. 2, pp. 582–589, Feb. 2018.

[24] H. Huang, Z. Shen, and A. A. Omar, "3-D absorptive frequency selective reflector for antenna radar cross section reduction," *IEEE Trans. Antennas Propag.*, vol. 65, no. 11, pp. 5908–5917, Nov. 2017.

[25] Q. Chen, M. Guo, D. Sang, Z. Sun, and Y. Fu, "RCS reduction of patch array antenna using anisotropic resistive metasurface," *IEEE Antennas Wireless Propag. Lett.*, vol. 18, no. 6, pp. 1223–1227, Jun. 2019.

[26] B. Zhang, L. Li, C. Jin, Q. Lv, and R. Mittra, "Wideband low RCS antenna based on hybrid absorptive-diffusive frequency selective reflector," *IEEE Access*, vol. 9, pp. 77863–77872, 2021.

[27] W. Yu, Y. Yu, W. Wang, X. H. Zhang, and G. Q. Luo, "Low-RCS and gain-enhanced antenna using absorptive/transmissive frequency selective structure," *IEEE Trans. Antennas Propag.*, vol. 69, no. 11, pp. 7912–7917, Nov. 2021.

[28] Y. Yu, W. Yu, G. Xie, J. Tong, and G. Q. Luo, "Wideband RCS reduction of slot array antenna utilizing 3-D absorptive frequency-selective structure," *IEEE Antennas Wireless Propag. Lett.*, vol. 21, no. 1, pp. 64–68, Jan. 2022.

[29] K. Zhang, R. Tan, Z. H. Jiang, Y. Huang, L. Tang, and W. Hong, "A compact, ultrawideband dual-polarized Vivaldi antenna with radar cross section reduction," *IEEE Antennas Wireless Propag. Lett.*, vol. 21, no. 7, pp. 1323–1327, Jul. 2022.

[30] P. Mei, X. Q. Lin, J. W. Yu, P. C. Zhang, and A. Boukarkar, "A low radar cross section and low profile antenna co-designed with absorbent frequency selective radome," *IEEE Trans. Antennas Propag.*, vol. 66, no. 1, pp. 409–413, Jan. 2018.

[31] M. M. Zargar, A. Rajput, K. Saurav, and S. K. Koul, "Low radar cross section dipole antenna integrated with absorptive frequency selective reflection structure," in *Proc. 16th Eur. Conf. Antennas Propag. (EuCAP)*, Mar. 2022, pp. 1–4.

[32] K. Saurav, D. Sarkar, and K. V. Srivastava, "CRLH unit-cell loaded multiband printed dipole antenna," *IEEE Antennas Wireless Propag. Lett.*, vol. 13, pp. 852–855, 2014.
[33] P. Alitalo, A. E. Culhaoglu, A. V. Osipov, S. Thurner, E. Kemptner, and S. A. Tretyakov, "Experimental characterization of a broadband transmission-line cloak in free space," *IEEE Trans. Antennas Propag.*, vol. 60, no. 10, pp. 4963–4968, Oct. 2012.
[34] M. M. Zargar, A. Rajput, K. Saurav, and S. K. Koul, "Frequency-selective rasorber based on high-Q Minkowski fractal-shaped resonator for realizing a low radar cross-section radiating system," *IEEE Trans. Electromagn. Compat.*, vol. 64, no. 5, pp. 1574–1584, Oct. 2022.

MEHRAN MANZOOR ZARGAR (Graduate Student Member, IEEE) received the B.Tech. degree in electronics and communication engineering from the University of Kashmir, Srinagar, Jammu and Kashmir, India, in 2014, and the M.Tech. degree in microelectronics from the National Institute of Technology Srinagar, in 2018. He is currently pursuing the Ph.D. degree in RF and microwave with the Department of Electrical Engineering, Indian Institute of Technology Jammu, India. His current research interest includes FSS-based rasorbers for RCS reduction. He currently serves as the Chair for IEEE AP-S Student Branch Chapter of IIT Jammu.

ARCHANA RAJPUT received the B.Tech. degree in electronics engineering from the Kamla Nehru Institute of Technology, Sultanpur, affiliated under Uttar Pradesh Technical University Lucknow, in 2009, the M.Tech. degree in microwave electronics from Delhi University, South Campus, in 2012, and the Ph.D. degree from the Department of Electrical Engineering, Indian Institute of Technology, Kanpur, India, in 2018.

She has worked as a Visiting Faculty at the Department of Electrical Engineering, Indian Institute of Technology Jammu, India. She is currently an Assistant Professor with the Department of Electronics and Communication Engineering, National Institute of Technology Srinagar, India. She has published several research papers in esteemed journals and conferences. One of her journal article titled design of a 2-D meta material cloak with minimum scattering using a quadratic transformation function has been featured on the Cover Page of *Journal of Applied Physics* (AIP). Her current research interests include transformation electromagnetics, cloaking/invisibility, metamaterials, antennas, and frequency selective surfaces.

KUSHMANDA SAURAV (Member, IEEE) received the B.E. degree in electronics and telecommunication from Bengal Engineering and Science University, Shibpur, India, in 2009, the M.Tech. degree in electronics and communication engineering from IIT Roorkee, India, in 2011, and the Ph.D. degree in electrical engineering from IIT Kanpur, India, in 2017. He worked as a Postdoctoral Fellow with the Royal Military College of Canada. He is currently an Assistant Professor with the Department of Electrical Engineering, IIT Jammu, India. He has published more than 70 research papers in esteemed journals and conferences. He has the experience of supervising M.Tech. and Ph.D. students and undertaking sponsored projects. His research interests include microwave and millimetre wave antennas and frequency selective surfaces. He has served as reviewers for IEEE, IET, and Wiley Journals. He is currently involved in the professional activities of the IEEE. He is currently the Faculty Advisor of IEEE MTTS and APS Student Branch Chapters of IIT Jammu.

SHIBAN K. KOUL (Life Fellow, IEEE) received the B.E. degree in electrical engineering from the Regional Engineering College, Srinagar, India, in 1977, and the M.Tech. and Ph.D. degrees in microwave engineering from the Indian Institute of Technology Delhi, New Delhi, India, in 1979 and 1983, respectively.

He served as the Deputy Director (strategy and planning) at IIT Delhi, from 2012 to 2016, and the Mentor Deputy Director (strategy and planning, international affairs) at IIT Jammu, from 2018 to 2021. He was the Chairperson of Astra Microwave Products Ltd., Hyderabad, from 2009 to 2019, and Dr. R. P. Shenoy Astra Microwave Chair Professor at IIT Delhi, from 2014 to 2019. He is currently an Emeritus Professor with the Indian Institute of Technology Delhi. He has authored/coauthored 570 research papers, 19 state-of-the art books, four book chapters, and two e-books. He holds 25 patents, six copyrights and one trademark. He has guided 30 Ph.D. thesis and more than 120 master's theses. He has successfully completed 151 major sponsored, consultancy, and technology development projects. His research interests include RF MEMS, high frequency wireless communication, microwave engineering, microwave passive and active circuits, device modeling, millimetre and sub-millimetre wave IC design, body area networks, flexible and wearable electronics, medical applications of sub-terahertz waves, and reconfigurable microwave circuits including miniaturized antennas.

Prof. Koul is a fellow of INAE and IETE. He served as a Distinguished Microwave Lecturer for IEEE MTT-S, from 2012 to 2014. He was a recipient of numerous awards including the IEEE MTT Society Distinguished Educator Award, in 2014, the Teaching Excellence Award from IIT Delhi, in 2012, the Indian National Science Academy (INSA) Young Scientist Award, in 1986, the Top Invention Award from the National Research Development Council for his contributions to the indigenous development of ferrite phase shifter technology, in 1991, the VASVIK Award for the development of Ka-band components and phase shifters, in 1994, the Ram Lal Wadhwa Gold Medal from the Institution of Electronics and Communication Engineers (IETE), in 1995, the Academic Excellence Award from the Indian Government for his pioneering contributions to phase control modules for Rajendra Radar, in 1998, the Shri Om Prakash Bhasin Award in the field of electronics and information technology, in 2009, the VASVIK Award for the contributions made to the area of Information, in 2012, and the Communication Technology (ICT) and M. N. Saha Memorial Award from IETE, in 2013. He is the Chief Editor of *IETE Journal of Research* and an Associate Editor of the *International Journal of Microwave and Wireless Technologies* (Cambridge University Press).